



This discussion paper is/has been under review for the journal Atmospheric Chemistry and Physics (ACP). Please refer to the corresponding final paper in ACP if available.

Mass-based hygroscopicity parameter interaction model and measurement of atmospheric aerosol water uptake

E. Mikhailov^{1,2}, V. Merkulov², S. Vlasenko², D. Rose¹, and U. Pöschl¹

¹Biogeochemistry Department, Max Planck Institute for Chemistry, Mainz, Germany

²Atmospheric Physics Department, Institute of Physics, St. Petersburg State University, St. Petersburg, Russia

Received: 21 October 2011 – Accepted: 31 October 2011 – Published: 18 November 2011

Correspondence to: E. Mikhailov (eugene.mikhailov@paloma.spbu.ru)

Published by Copernicus Publications on behalf of the European Geosciences Union.

Mass-based hygroscopicity parameter interaction model

E. Mikhailov et al.

[Title Page](#)

[Abstract](#)

[Introduction](#)

[Conclusions](#)

[References](#)

[Tables](#)

[Figures](#)

◀

▶

[Back](#)

[Close](#)

[Full Screen / Esc](#)

[Printer-friendly Version](#)

[Interactive Discussion](#)



Abstract

In this study we derive and apply a mass-based hygroscopicity parameter interaction model for efficient description of concentration-dependent water uptake by atmospheric aerosol particles. The model approach builds on the single hygroscopicity parameter model of Petters and Kreidenweis (2007). We introduce an observable mass-based hygroscopicity parameter κ_m , which can be deconvoluted into a dilute intrinsic hygroscopicity parameter ($\kappa_{m,\infty}$) and additional self- and cross-interaction parameters describing non-ideal solution behavior and concentration dependencies of single- and multi-component systems.

For sodium chloride, the κ_m -interaction model (KIM) captures the observed concentration and humidity dependence of the hygroscopicity parameter and is in good agreement with an accurate reference model based on the Pitzer ion-interaction approach (Aerosol Inorganic Model, AIM). For atmospheric aerosol samples collected from boreal rural air and from pristine tropical rainforest air (secondary organic aerosol) we present first mass-based measurements of water uptake over a wide range of relative humidity (1–99 %) obtained with a new filter-based differential hygroscopicity analyzer (FDHA) technique. By application of KIM to the measurement data we can distinguish three different regimes of hygroscopicity in the investigated aerosol samples: (I) A quasi-eutonic regime at low relative humidity ($\lesssim 60\% \text{ RH}$) where the solutes co-exist in an aqueous and non-aqueous phase; (II) a gradually deliquescent regime at intermediate humidity ($\sim 60\% \text{--} 90\% \text{ RH}$) where different solutes undergo gradual dissolution in the aqueous phase; and (III) a dilute regime at high humidity ($\gtrsim 90\% \text{ RH}$) where the solutes are fully dissolved approaching their dilute intrinsic hygroscopicity. The characteristic features of the three hygroscopicity regimes are similar for both samples, while the RH threshold values vary as expected for samples of different chemical composition.

In each regime, the concentration dependence of κ_m can be described by a simple KIM model equation based on observable mass growth factors and six fit parameters

Mass-based hygroscopicity parameter interaction model

E. Mikhailov et al.

[Title Page](#)

[Abstract](#)

[Introduction](#)

[Conclusions](#)

[References](#)

[Tables](#)

[Figures](#)

◀

▶

◀

▶

[Back](#)

[Close](#)

[Full Screen / Esc](#)

[Printer-friendly Version](#)

[Interactive Discussion](#)



summarizing the combined effects of the dilute intrinsic hygroscopicity and interaction parameters of all involved chemical components. One of the fit parameters represents $\kappa_{m,\infty}$ and can be used to predict CCN activation diameters as a function of water vapor supersaturation. For sodium chloride reference particles as well as for pristine rainforest aerosols consisting mostly of secondary organic matter, we obtained good agreement between the predicted and measured critical diameters of CCN activation.

The application of KIM and mass-based measurement techniques shall help to bridge gaps in the current understanding of water uptake by atmospheric aerosols: (1) the gap between hygroscopicity parameters determined by HTDMA (hygroscopicity tandem differential mobility analyzer) or FDHA measurements under sub-saturated conditions and by CCN measurements at water vapor supersaturation, and (2) the gap between the results of simplified single parameter models widely used in atmospheric or climate science and the results of complex multi-parameter ion- and molecule-interaction models frequently used in physical chemistry and thermodynamics (AIM, E-AIM, UNIFAC, AIOMFAC etc.).

1 Introduction

The interaction of aerosol particles with water vapor is among the central issues of current research in atmospheric and climate science, and numerous studies have investigated the hygroscopicity of aerosol particles and their ability to serve as cloud condensation nuclei (CCN). Köhler theory is the main tool to describe the hygroscopic growth of particles as a function of relative humidity (e.g., Pruppacher and Klett, 2000; Seinfeld and Pandis, 2006), and various types of Köhler models have been developed and applied for the analysis of laboratory and field measurement results as well as in numerical models of the atmosphere and climate (e.g., Junge and McLaren, 1971; Fitzgerald, 1973; Shulman et al., 1996; Kulmala et al., 1997; Laaksonen et al., 1998; Raymond and Pandis, 2003; Bilde and Svenningsson, 2004; Mikhailov et al., 2004; Huff-Hartz et al., 2005; Kreidenweis et al., 2005; Topping et al., 2005; Svenningsson

Mass-based hygroscopicity parameter interaction model

E. Mikhailov et al.

[Title Page](#)

[Abstract](#)

[Introduction](#)

[Conclusions](#)

[References](#)

[Tables](#)

[Figures](#)

[◀](#)

[▶](#)

[Back](#)

[Close](#)

[Full Screen / Esc](#)

[Printer-friendly Version](#)

[Interactive Discussion](#)



Mass-based hygroscopicity parameter interaction model

E. Mikhailov et al.

[Title Page](#)[Abstract](#)[Introduction](#)[Conclusions](#)[References](#)[Tables](#)[Figures](#)[◀](#)[▶](#)[Back](#)[Close](#)[Full Screen / Esc](#)[Printer-friendly Version](#)[Interactive Discussion](#)

et al., 2006; Fountoukis and Nenes, 2007; Petters and Kreidenweis, 2007; Rose et al., 2008; Mikhailov et al., 2009; Ruehl et al., 2010; Metzger et al., 2011; and references therein).

A central aim of hygroscopicity measurements and studies that discuss different assumptions for parameters used in the Köhler equation is to relate the critical supersaturation of CCN activation to the hygroscopic growth factors observed at subsaturated conditions (e.g., Rissler et al., 2004; Kreidenweis et al., 2005; Mochida et al., 2006; Petters and Kreidenweis, 2007; Wex et al., 2008; Gunthe et al., 2009; Petters et al., 2009; Good et al., 2010a,b; Irwin et al., 2010; Roberts et al., 2010; Cerully et al., 2011; Duplissy et al., 2011; Fors et al., 2011). For this purpose, Petters and Kreidenweis (2007) proposed a single-parameter Köhler model where the hygroscopicity parameter κ provides a volume-based measure of aerosol water uptake characteristics and CCN activity. For water soluble organic and inorganic compounds, the relative differences between κ values derived from CCN and growth factor measurements are usually less than 30 % and can be explained by non-ideal behavior of concentrated solutions (e.g., Wex et al., 2008; Mikhailov et al., 2009). For particles containing sparingly soluble compounds, however, the differences can increase by a factor of 5 or more (Petters and Kreidenweis, 2007). To bridge the gap between κ values observed under subsaturated and supersaturated conditions, Petters and Kreidenweis (2008) proposed a pseudo-two-component κ -Köhler model where sparingly soluble compounds gradually enter the solution with increasing dilution and relative humidity. The practical applicability of volume based hygroscopicity models, however, is often limited by deviations from volume-additivity and by the effects of capillary condensation and restructuring of porous and irregularly shaped particles (e.g., Krämer et al., 2000; Colberg et al., 2004; Mikhailov et al., 2004; Gysel et al., 2004; Marcolli and Krieger, 2006; Sjogren et al., 2007; Zardini et al., 2008; Mifflin et al., 2009; Mikhailov et al., 2009; Wang et al., 2010; Smith et al., 2011).

In this study we introduce a mass-based hygroscopicity parameter κ_m building on the single hygroscopicity parameter of Petters and Kreidenweis (2007), and we develop a

κ_m -interaction model (KIM) to describe non-ideal solution behavior and concentration dependencies of single- and multi-component systems. We demonstrate that the KIM approach can capture and reproduce the characteristics of water uptake by pure reference substances as well as atmospheric aerosol samples under sub- and supersaturated conditions.

2 Theory

2.1 Volume-based hygroscopicity parameter κ

The Köhler theory relates the water vapor saturation ratio ($s_w = \text{RH}/100\%$) to the water activity (a_w), the partial molar volume of water (\bar{V}_w), the surface tension (σ), and the diameter (D) of a spherical aqueous droplet under equilibrium conditions (e.g., Pruppacher and Klett, 2000; Seinfeld and Pandis, 2006):

$$s_w = a_w \exp \left(\frac{4\sigma \bar{V}_w}{RTD} \right) \quad (1)$$

where R is the universal gas constant and T is the temperature. Note that all symbols frequently used in this manuscript are also explained in Table 1.

According to Petters and Kreidenweis (2007), the hygroscopic growth of aerosol particles can be efficiently approximated by a simplified version of Eq. (1), the so-called κ -Köhler equation:

$$s_w = a_w \exp \left(\frac{4\sigma_w M_w}{RT \rho_w D} \right) = \left(\frac{\kappa}{G_D^3 - 1} + 1 \right)^{-1} \exp \left(\frac{4\sigma_w M_w}{RT \rho_w G_D D_d} \right) \quad (2)$$

Here M_w , σ_w , and ρ_w are the molar mass, surface tension, and density of pure water, respectively. The diameter growth factor G_D is defined as the ratio between the

Mass-based hygroscopicity parameter interaction model

E. Mikhailov et al.

[Title Page](#)

[Abstract](#)

[Introduction](#)

[Conclusions](#)

[References](#)

[Tables](#)

[Figures](#)

◀

▶

◀

▶

[Back](#)

[Close](#)

[Full Screen / Esc](#)

[Printer-friendly Version](#)

[Interactive Discussion](#)



volume equivalent diameters of the aqueous droplet and of the dry aerosol particle ($G_D = D/D_d$).

The hygroscopicity parameter κ relates the volume of the dry aerosol particle (V_d) to the volume of water (V_w) and the activity of water (a_w) in the aqueous droplet:

$$5 \quad \frac{1}{a_w} = 1 + \kappa \frac{V_d}{V_w} \quad (3)$$

$$a_w = \left(\frac{\kappa}{G_D^3 - 1} + 1 \right)^{-1} \quad (4)$$

Equations (2)–(4) are commonly used to determine effective hygroscopicity parameters from HTDMA and CCN measurements (e.g.: Petters and Kreidenweis, 2007; Petters et al., 2009; Gunthe et al., 2009; Mikhailov et al., 2009; Carrico et al., 2010; Rose et al.,

10 2010, 2011; Duplissy et al., 2011 and references therein). In the analysis of laboratory and field measurement data it is often assumed that measured mobility equivalent diameters (D, D_d) can be regarded as volume equivalent diameters, and that the volume of the aqueous droplet is a linear addition of the dry particle volume and the volume of the amount of water taken up into the wet particle ($V = V_d + V_w$; “volume additivity assumption”). The limitations of these assumptions for HTDMA and CCN experiments have been outlined and discussed in earlier studies (e.g., Krämer et al., 2000; Gysel et al., 2002; Rose et al. 2008; Mikhailov et al., 2004, 2009; and references therein).

15 Depending on aerosol particle sources and properties, the deviations from ideality can range from a few percent up to a factor of 2 or more.

20 For an individual solute (i), the hygroscopicity parameter can be related to the molar mass (M_i), density (ρ_i), and the van't Hoff factor or effective dissociation number (J_i) of the solute:

$$\kappa_i = J_i \frac{\rho_i/M_i}{\rho_w/M_w} \quad (5)$$

Mass-based hygroscopicity parameter interaction model

E. Mikhailov et al.

[Title Page](#)

[Abstract](#)

[Introduction](#)

[Conclusions](#)

[References](#)

[Tables](#)

[Figures](#)

◀

▶

◀

▶

[Back](#)

[Close](#)

[Full Screen / Esc](#)

[Printer-friendly Version](#)

[Interactive Discussion](#)

Mass-based hygroscopicity parameter interaction model

E. Mikhailov et al.

Title Page	
Abstract	Introduction
Conclusions	References
Tables	Figures
	
Back	Close
Full Screen / Esc	
Printer-friendly Version	
Interactive Discussion	

Thus, κ_i can be regarded as an effective molar density of ions or molecules in the solute normalized by the molar density of water ($\rho_w/M_w \approx 55 \text{ mol L}^{-1}$), which has been designated as “effective Raoult parameter” or “intrinsic hygroscopicity” of the solute (Mikhailov et al., 2009; Sullivan et al., 2009).

In concentrated solutions, κ_i is usually concentration-dependent (Mikhailov et al., 2009), but under dilute conditions it approaches a substance-specific fixed value which we designate as the “dilute intrinsic hygroscopicity”, $\kappa_{i,\infty}$. This parameter is easy to calculate from tabulated values of J_i for dilute aqueous solutions, and it can be used as a basis for describing the concentration dependence of hygroscopicity parameters as detailed below (Sect. 2.3).

2.2 Mass-based hygroscopicity parameter κ_m

In analogy to the volume-based hygroscopicity parameter (Eq. 3), we define a mass-based hygroscopicity parameter κ_m :

$$\frac{1}{a_w} = 1 + \kappa_m \frac{m_d}{m_w} \quad (6)$$

where m_d is the mass of the dry particle material and m_w is the mass of water in the wet particle (aqueous droplet).

From Eqs. (3) and (6) follows

$$\kappa_m = \kappa \frac{\rho_w}{\rho_d} \quad (7)$$

where ρ_d is the effective density of the dry particle material. Thus, the knowledge of ρ_d enables conversion of κ into κ_m and vice versa. On the other hand, independent measurements of κ and κ_m enable the determination of ρ_d .

The mass-based dilute intrinsic hygroscopicity, $\kappa_{m,i,\infty}$, follows from Eqs. (5) and (7); it is simply the van't Hoff factor (J_i) scaled by the ratio of the molar masses of water

and solute:

$$\kappa_{m,i,\infty} = J_i \frac{M_w}{M_i} \quad (8)$$

By defining the mass growth factor G_m as

$$G_m = \frac{m_w + m_d}{m_d} \quad (9)$$

5 and combining Eqs. (9) and (6) we obtain

$$a_w = \left(\frac{\kappa_m}{G_m - 1} + 1 \right)^{-1} \quad (10)$$

The mass-based relation between water activity and particle hygroscopicity specified in Eq. (10) is equivalent to the volume based formulation in Eq. (4). Due to mass conservation, however, the practical applicability of Eq. (10) and the precision of related 10 parameters determined in mass-based experiments is not affected by deviations from spherical geometry and volume additivity that usually limit the applicability and precision of volume-based parameters determined in mobility diameter-based HTDMA and CCN experiments (e.g.: Krämer et al., 2000; Gysel et al., 2002, 2004; Rose et al., 2008; Mikhailov et al. 2004, 2009; Wang et al., 2010; and references therein).

15 The mass-based definition of the hygroscopicity parameter κ_m (Eq. 6) avoids a complication that occurs in the volume-based definition of κ (Eq. 3): the theoretical distinction and practical determination of specific volume vs. partial specific volume (alias molar vs. partial molar volume) of water and solute in a solution droplet. This distinction had not been addressed and specified in the original volume-based definition of 20 κ (Petters and Kreidenweis, 2007), but it is relevant in systems where the volumes of mixed components are not linearly additive.

If the densities of the dry solute and of the solution are known, the masses of dry particles and aqueous droplets can be easily converted into volume equivalent diameters:

Mass-based
hygroscopicity
parameter interaction
model

E. Mikhailov et al.

[Title Page](#)

[Abstract](#)

[Introduction](#)

[Conclusions](#)

[References](#)

[Tables](#)

[Figures](#)

◀

▶

[Back](#)

[Close](#)

[Full Screen / Esc](#)

[Printer-friendly Version](#)

[Interactive Discussion](#)



Mass-based hygroscopicity parameter interaction model

E. Mikhailov et al.

[Title Page](#)

[Abstract](#)

[Introduction](#)

[Conclusions](#)

[References](#)

[Tables](#)

[Figures](#)

[◀](#)

[▶](#)

[◀](#)

[▶](#)

[Back](#)

[Close](#)

[Full Screen / Esc](#)

[Printer-friendly Version](#)

[Interactive Discussion](#)



$D_d^3 = 6m_d/(\pi\rho_d)$, $D^3 = 6G_m m_d/(\pi\rho)$, and $D = D_d (G_m \rho_d/\rho)^{1/3}$, where ρ is the density of the aqueous solution droplet. For dilute aqueous solution droplets with $\rho \approx \rho_w$ follows

$$D = D_d \left(G_m \frac{\rho_d}{\rho_w} \right)^{1/3} \quad (11)$$

By inserting Eqs. (10) and (11) in Eq. (2), we obtain an approximate mass-based κ_m -Köhler equation:

$$s_w = \left(\frac{\kappa_m}{G_m - 1} + 1 \right)^{-1} \exp \left(\frac{4\sigma_w M_w}{RT \rho_w D_d} \left[\frac{\rho_w}{\rho_d G_m} \right]^{1/3} \right) \quad (12)$$

The critical mass growth factor ($G_{m,c}$) and the critical water vapor saturation ratio ($s_{w,c}$) for the CCN activation of an aerosol particle with dry diameter D_d and hygroscopicity κ_m correspond to the maximum value of s_w according to Eq. (12) ($ds_w/dG_m = 0$):

$$G_{m,c} = \left(\frac{3\kappa_m D_d}{A} \right)^{3/2} \left(\frac{\rho_d}{\rho_w} \right)^{1/2} \quad (13)$$

$$s_{w,c} = \exp \left(\frac{2}{3} \left[\frac{A}{D_d} \right]^{3/2} \left[\frac{\rho_w}{3\kappa_m \rho_d} \right]^{1/2} \right) \quad (14)$$

with

$$A = \frac{4\sigma_w M_w}{RT \rho_w}$$

Exponential series expansion, cancellation of higher order terms, and rearrangement of Eq. (14) lead to the following approximate relation between the critical dry diameter $D_{d,c}$ and the supersaturation of CCN activation ($S_w = (s_w - 1) \cdot 100\%$):

$$D_{d,c} = A \cdot \left(\frac{4\rho_w}{27\kappa_m \rho_d} \right)^{1/3} \left(\frac{S_w}{100} \right)^{-2/3} = \beta \cdot S_w^{-2/3} \quad (15)$$

with

$$\beta = A \cdot \left(\frac{4\rho_w}{27\kappa_m \rho_d} \right)^{\frac{1}{3}} \left(\frac{1}{100} \right)^{-\frac{2}{5}}$$

2.3 Hygroscopicity parameter interaction model (KIM)

In analogy to Petters and Kreidenweis (2008, Eq. 10), the mass-based hygroscopicity

- ⁵ parameter of a multi-component particle can be approximated by a simple mixing rule that builds on the Zdanovskii-Stokes-Robinson (ZSR) approach (Stokes and Robinson, 1966; Seinfeld and Pandis 2006):

$$\kappa_m = \sum_i f_i \kappa_{m,i} H(y_{m,i}) \quad (16)$$

$$H(y_{m,i}) = \begin{cases} y_{m,i} & \text{if } y_{m,i} < 1 \text{ (partly dissolved)} \\ 1 & \text{if } y_{m,i} \geq 1 \text{ (fully dissolved)} \end{cases}$$

$$y_{m,i} = (G_m - 1) C_{m,i} / f_i$$

Here f_i is the dry mass fraction of the solute component i , $C_{m,i}$ is the solubility of the solute in water (mass of dissolved compound i per unit mass of water under equilibrium conditions), and $H(y_{m,i})$ is the relative fraction of component i that is actually dissolved in the aqueous phase. Accordingly, water insoluble components with $\kappa_m \approx 0$ do not contribute to the overall particle hygroscopicity. For completely dissolved particles, all values of $y_{m,i}$ equal unity, and κ_m is given by the simple relation

$$\kappa_m = \sum_i f_i \kappa_{m,i} \quad (17)$$

Note that in Eqs. (16) and (17) the hygroscopicity parameters of individual chemical components $\kappa_{m,i}$ are weighted by the corresponding mass fractions, f_i , which are usually easier to determine than volume fractions. Due to the difficulties involved in obtaining correct density estimates for mixtures of organic and inorganic compounds in

Mass-based hygroscopicity parameter interaction model

E. Mikhailov et al.

[Title Page](#)

[Abstract](#)

[Introduction](#)

[Conclusions](#)

[References](#)

[Tables](#)

[Figures](#)

[◀](#)

[▶](#)

[◀](#)

[▶](#)

[Back](#)

[Close](#)

[Full Screen / Esc](#)

[Printer-friendly Version](#)

[Interactive Discussion](#)



Mass-based hygroscopicity parameter interaction model

E. Mikhailov et al.

[Title Page](#)

[Abstract](#)

[Introduction](#)

[Conclusions](#)

[References](#)

[Tables](#)

[Figures](#)

[◀](#)

[▶](#)

[◀](#)

[▶](#)

[Back](#)

[Close](#)

[Full Screen / Esc](#)

[Printer-friendly Version](#)

[Interactive Discussion](#)

atmospheric aerosol particles, many recent studies applying a hygroscopicity parameter mixing rule used mass fractions as a proxy for volume fractions (e.g., Kreidenweis 2008; Gunthe et al., 2009, 2011; Pringle et al., 2010; Rose et al., 2011).

In the highly dilute solution droplets usually formed at high RH and upon CCN activation, the hygroscopicity parameters of individual solute components ($K_{m,i}$) approach the dilute-intrinsic hygroscopicity values $\kappa_{m,i,\infty}$ that can be estimated using Eq. (8) and inserted in Eq. (16) or Eq. (17), respectively.

In the highly concentrated solutions formed at low RH, however, the hygroscopicity of aerosol particles does not always follow the simple ZSR approach (ideal mixing). 10 Interactions between solute ions and molecules can lead to either higher or lower solubilities and hygroscopicity parameters as compared to single-component and dilute solutions (Marcolli et al. 2004; Marcolli and Krieger, 2006; Mikhailov et al., 2009).

To describe the non-ideal behavior of concentrated solutions, we propose a hygroscopicity parameter interaction model, briefly κ_m -interaction model (KIM), that combines dilute intrinsic hygroscopicity parameters with additional terms of cross- or self-interaction between molecular and ionic species:

$$\kappa_m = \sum_i K_{m,i} \quad (18)$$

where the mass-weighted hygroscopicity parameter $K_{m,i}$ for each component is defined by

$$20 \quad K_{m,i} = \begin{cases} (\kappa_{m,i,\infty} + \delta\kappa_{m,ij} + \delta\kappa_{m,ii})(G_m - 1)C_{m,i} & \text{if } (G_m - 1)C_{m,i} < f_i \text{ (partly dissolved)} \\ (\kappa_{m,i,\infty} + \delta\kappa_{m,ij} + \delta\kappa_{m,ii})f_i & \text{if } (G_m - 1)C_{m,i} \geq f_i \text{ (fully dissolved)} \end{cases} \quad (19)$$

Here $\delta\kappa_{m,ij}$ and $\delta\kappa_{m,ii}$ are defined as incremental hygroscopicity terms accounting for cross- and self-interactions of molecular and ionic species, respectively. In analogy to other physico-chemical parameters of atmospheric aerosols and aqueous solution droplets (Finlayson-Pitts and Pitts, 2000), the concentration dependence of the

Mass-based hygroscopicity parameter interaction model

E. Mikhailov et al.

incremental terms $\delta\kappa_{m,ij}$ and $\delta\kappa_{m,ii}$ can be described by:

$$\begin{aligned}\delta\kappa_{m,ij} &= c_{m,i} \sum_{j \neq i} \alpha_{ij} c_{m,j} \\ \delta\kappa_{m,ii} &= \alpha_{ii} c_{m,i}^2\end{aligned}\quad (20)$$

Here α_{ij} and α_{ii} are cross- and self-interaction coefficients, respectively; $c_{m,i}$ and $c_{m,j}$ are the mass concentrations of individual components (i, j) in the aqueous solution expressed here as mass of solute per unit mass of water. Depending on the nature of solute interaction, the interaction coefficients and the resulting incremental hygroscopicity terms can assume positive or negative values.

The mass concentration $c_{m,i}$ can be calculated either from the solubility $C_{m,i}$ (if component i is only partially dissolved) or from the dry mass fraction f_i (if component i is fully dissolved):

$$c_{m,i} = \begin{cases} C_{m,i} & \text{if } (G_m - 1)C_{m,i} < f_i \\ f_i/(G_m - 1) & \text{if } (G_m - 1)C_{m,i} \geq f_i \end{cases} \quad (21)$$

For a particle consisting of an aqueous phase (aq) and a non-aqueous phase (na), Eqs. (18) to (21) can be combined into:

$$\begin{aligned}\kappa_m &= \sum_{i \in \text{na}} \left(\kappa_{m,i,\infty} + C_{m,i} \left[\sum_{\substack{j \in \text{aq}, \\ j \neq i}} \alpha_{ij} \frac{f_j}{G_m - 1} + \sum_{\substack{j \in \text{na}, \\ j \neq i}} \alpha_{ij} C_{m,j} \right] + \alpha_{ii} C_{m,i}^2 \right) (G_m - 1) C_{m,i} + \\ &\quad \sum_{i \in \text{aq}} \left(\kappa_{m,i,\infty} + \frac{f_i}{G_m - 1} \left[\sum_{\substack{j \in \text{aq}, \\ j \neq i}} \alpha_{ij} \frac{f_j}{G_m - 1} + \sum_{\substack{j \in \text{na}, \\ j \neq i}} \alpha_{ij} C_{m,j} \right] + \alpha_{ii} \frac{f_i^2}{(G_m - 1)^2} \right) f_i\end{aligned}\quad (22)$$

Mass-based hygroscopicity parameter interaction model

E. Mikhailov et al.

[Title Page](#)

[Abstract](#)

[Introduction](#)

[Conclusions](#)

[References](#)

[Tables](#)

[Figures](#)

[◀](#)

[▶](#)

[◀](#)

[▶](#)

[Back](#)

[Close](#)

[Full Screen / Esc](#)

[Printer-friendly Version](#)

[Interactive Discussion](#)

where

$$i \in \text{na}, \text{ if } (G_m - 1)C_{m,i} < f_i \quad (23)$$

$$i \in \text{aq}, \text{ if } (G_m - 1)C_{m,i} \geq f_i$$

Here the designation $i \in \text{na}$ means that component i is only partially dissolved in the aqueous phase, while the designation $i \in \text{aq}$ refers to a component that is fully dissolved in the aqueous phase.

For $i \in \text{na}$ the aqueous phase concentration $c_{m,i}$ depends on $C_{m,i}$, and for $i \in \text{aq}$ the aqueous phase concentration $c_{m,i}$ depends on G_m and f_i as specified in Eq. (21).

In multi-component systems, the solubility of an individual component $C_{m,i}$ in the mixture is not necessarily the same as the solubility of the component in pure water, $C_{m,w,i}$ (single-component system). Interactions between different substances can increase or decrease the solubility of individual components (Marcolli et al., 2004; Marcolli and Krieger, 2006). The influence of multiple solutes on the solubility of individual components can be described according to the Setschenov equation (Setschenov, 1889):

$$\frac{C_{m,i}}{C_{m,w,i}} = \exp \left(\sum_{j \in \text{na}} \eta_{ij} C_{m,j} + \sum_{j \in \text{aq}} \eta_{ij} \left[\frac{f_j}{G_m - 1} \right] \right) \quad (24)$$

where η_{ij} is the salting out constant.

If all substances co-exist in the non-aqueous phase, the aqueous phase concentration of each component is given by the eutonic solubility, $C_{m,e,i}$. In this case, Eq. (22) can be reduced to

$$\kappa_m = \sum_{i \in \text{na}} \left(\kappa_{m,i,\infty} + C_{m,e,i} \sum_{\substack{j \in \text{na}, \\ j \neq i}} \alpha_{ij} C_{m,e,j} + \alpha_{ii} C_{m,e,i}^2 \right) (G_m - 1) C_{m,e,i} \quad (25)$$

If all substances are completely dissolved, Eq. (22) can be reduced to

$$\kappa_m = \sum_{i \in \text{eq}} \left(\kappa_{m,i,\infty} + \frac{f_i}{G_m - 1} \sum_{\substack{j \in \text{eq}, \\ j \neq i}} \alpha_{ij} \frac{f_j}{G_m - 1} + \alpha_{ii} \frac{f_i^2}{(G_m - 1)^2} \right) f_i \quad (26)$$

In case of dilute solutions ($G_m \gg 1$), the relative importance of the incremental hygroscopicity terms decreases and Eq. (26) can be further reduced to Eq. (17).

- 5 For a single component system with $f_i = 1$, $f_j = 0$, and $\alpha_{ii} = \alpha$, Eq. (22) can be reduced to

$$\kappa_m = (\kappa_{m,\infty} + \alpha C_m^2)(G_m - 1)C_m \quad \text{if } (G_m - 1)C_m < 1 \text{ (partly dissolved)} \quad (27)$$

$$\kappa_m = \kappa_{m,\infty} + \frac{\alpha}{(G_m - 1)^2} \quad \text{if } (G_m - 1)C_m \geq 1 \text{ (fully dissolved)} \quad (28)$$

Eq. (28) can be combined with Eqs. (8), (10), and with the relation

$$10 \quad G_m - 1 = c_m^{-1} = (\mu M)^{-1} \quad (29)$$

to obtain an explicit expression of water activity in the aqueous solution of a fully dissolved single solute with molar mass M , molality μ , and van't Hoff factor J :

$$a_w = \left(1 + \kappa_{m,\infty} c_m + \alpha c_m^3 \right)^{-1} = \left(1 + J \mu M_w + \alpha (\mu M)^3 \right)^{-1} \quad (30)$$

This expression represents a middle way between the simplistic assumption of a constant single hygroscopicity parameter and the complex multi-parameter models like AIM (Aerosol Inorganics Model; e.g., Wexler and Clegg, 2002; <http://www.aim.env.uea.ac.uk/aim/aim.php>), E-AIM (Extended-AIM; e.g., Clegg et al., 2001; Clegg and Seinfeld, 2006a,b), UNIFAC, or AIOMFAC (e.g., Fredenslund et al., 1975; Zuernd et al., 2011) typically using more than five semi-empirical parameters for a single solute system. For the reasons outlined above (mass conservation vs. volume non-additivity)

Title Page

Abstract

Introduction

Conclusions

References

Tables

Figures

|◀

▶|

◀

▶

Back

Close

Full Screen / Esc

Printer-friendly Version

Interactive Discussion

Mass-based hygroscopicity parameter interaction model

E. Mikhailov et al.

[Title Page](#)

[Abstract](#)

[Introduction](#)

[Conclusions](#)

[References](#)

[Tables](#)

[Figures](#)

◀

▶

◀

▶

[Back](#)

[Close](#)

[Full Screen / Esc](#)

[Printer-friendly Version](#)

[Interactive Discussion](#)



the more detailed solute interaction models are generally also mass based rather than volume based.

Nevertheless, the hygroscopicity parameter interaction approach presented in this study can also be translated into analogous volume-based formulations based on the equivalence of κ_m and κ (Eq. 7). For example, the single component solution Eq. (28) can be rewritten as

$$\kappa_i = \kappa_{i,\infty} + \frac{\chi_{ii}}{(G_D^3 - 1)^2} \quad (31)$$

where χ_{ii} is a volume-based self-interaction coefficient.

3 Experiments

10 3.1 Aerosol filter sampling

Atmospheric aerosol samples were collected at a pristine tropical rainforest site and at a rural boreal site as specified in Table 2. The tropical sample was collected during the Amazonian Aerosol Characterization Experiment in February 2008 (AMAZE-08, Martin et al., 2010) at the rainforest research station TT34 near Manaus, Brazil (AMAZE sample). The boreal sample was collected in the rural environment of the Institute of Physics at Petrodvoretz near Saint-Petersburg, Russia, in May 2009 (SPB sample). The particles were collected by passing an air flow of 20 L min^{-1} consequently through a $1\text{ }\mu\text{m}$ cyclone (URG-2000-30EHB) and a 47 mm Teflon-coated glass fiber filter (Pallflex T60A20, Pall, Germany).

Reference aerosol particles were generated by nebulization of aqueous solution of sodium chloride (mass fraction 0.1 %) prepared by dissolving NaCl (Merck, >99.5 %) in deionized water ($18.2\text{ M}\Omega\text{ cm}$, Milli Q plus 185, Millipore). The sampling equipment on the filter and procedures were the same as applied for the atmospheric aerosol samples and the modal diameter of the aerosol mass size distribution was $\sim 350\text{ nm}$, which

implies that the Kelvin effect can be neglected ($RH = a_w$, relative deviations <1%). Usually the modal diameter of atmospheric aerosol mass size distributions is of similar magnitude or higher (e.g., ~250 nm for accumulation mode particles and ~3 µm for coarse mode particles during AMAZE-08; Pöschl et al. 2010). Thus we assume
5 $a_w = RH/(100\%)$ in this study unless mentioned otherwise.

3.2 Water uptake measurements

Mass-based water uptake measurements were performed with a filter-based differential hygroscopicity analyzer (FDHA) using the atmospheric aerosol filter samples and a sodium chloride reference sample collected as described above. Circular aliquots of
10 13 mm diameter were cut from the aerosol loaded filters and mounted in the FDHA system shown in Fig. 1. Details of the experimental setup and calibration are described elsewhere (Mikhailov et al., 2011); the operating principles are briefly outlined below.

In the FDHA system, the carrier gas (helium) was humidified with a bubbler (T_1), equilibrated in a saturator ($T_2 < T_1$), and then passed through a pair of differential measurement cells ($T_3 > T_2$). The reference cell contains a clean filter aliquot; the other cell contains the aerosol loaded filter aliquot. The mass of water taken up by the aerosol particles on the loaded filter aliquot was determined by a differential katharometer and recorded by an analog-digital converter and a personal computer. The measurement uncertainties depend on the weighing accuracy of dry particle mass (aerosol loading), absorbed water mass (aerosol hygroscopicity), and water vapor measurement precision of the katharometer (Mikhailov et al., 2011). In this study, the largest uncertainties in the determination of mass growth factors, G_m (Eq. 9) were associated with the AMAZE sample: ~1 % at 30 % RH and ~8 % at 99 % RH. The relative humidity of the FDHA water uptake measurement is determined from the temperature ratio between the water vapor saturator (T_2) and the measurement cells (T_3) using empirical formulas recommended by the World Meteorological Organization (Flatau et al., 1992). The accuracy at 99 % RH was $\pm 0.06\%$ RH, resulting from accurate temperature control using a double-wall copper housing with forced thermal insulation and precise
20
25

temperature measurements ($\pm 0.01^\circ \text{C}$, 42905-Pt100; KELVIMAT 4306, Burster). The water uptake experiments were performed in two modes: hydration = increasing RH; dehydration = decreasing RH.

4 Measurement results and discussion

5 4.1 Sodium chloride reference sample

Figure 2 shows the mass growth factors observed for sodium chloride as a function of relative humidity. Upon hydration, the NaCl sample exhibited a stepwise deliquescence transition at $\text{RH}_d = 75\text{--}76\%$ (Fig. 2a), which is in good agreement with literature data ($\text{RH}_d = 75.3\%$; Tang and Munkelwitz, 1993). From the mass growth factor measured right after the deliquescence transition, i.e., at $\text{RH} = 76\%$, we calculated the effective solubility using the relation $C_m = 1/(G_m - 1)$ (Eq. 29). The obtained value of $0.36 \pm 0.02 \text{ g g}^{-1}$ is in good agreement with literature data (Clarke and Glew, 1985; Marcolli et al., 2004; Stephen and Stephen, 1963). Upon dehydration, efflorescence of the solution droplets occurred over an RH range of 65–40 %.

15 The observation of a transition range rather than a sharp threshold value of RH can be explained by inhomogeneities and polydispersity of the investigated particles, whereby larger particles are likely to effloresce at higher RH. The model line shown in Fig. 2a demonstrates good agreement between the measurement data and the Aerosol Inorganic Model (AIM, Clegg et al. 1998), which is based on the Pitzer ion-interaction approach and can be regarded as an accurate reference model (Rose et al., 2008; 20 Mikhailov et al., 2009). For the calculation of mass growth factors from the generic AIM model output data we used Eq. (29).

25 Figure 2b shows the mass-based hygroscopicity parameter (κ_m) for NaCl as a function of the mass growth factor. The κ_m values were calculated by inserting the data pairs of G_m and a_w in Eq. (10) assuming $a_w = \text{RH}/(100\%)$ as explained in Sect. 2.1. The simple κ_m -interaction model for single solute systems (KIM, Eq. 28) was applied

Mass-based hygroscopicity parameter interaction model

E. Mikhailov et al.

[Title Page](#)

[Abstract](#)

[Introduction](#)

[Conclusions](#)

[References](#)

[Tables](#)

[Figures](#)

◀

▶

◀

▶

[Back](#)

[Close](#)

[Full Screen / Esc](#)

[Printer-friendly Version](#)

[Interactive Discussion](#)

Mass-based hygroscopicity parameter interaction model

E. Mikhailov et al.

[Title Page](#)

[Abstract](#)

[Introduction](#)

[Conclusions](#)

[References](#)

[Tables](#)

[Figures](#)

[◀](#)

[▶](#)

[◀](#)

[▶](#)

[Back](#)

[Close](#)

[Full Screen / Esc](#)

[Printer-friendly Version](#)

[Interactive Discussion](#)



to fit the measurement data points for fully dissolved NaCl (solid black line). The best fit parameter values and standard errors are $\kappa_{m,\infty} = 0.59 \pm 0.01$ and $\alpha = 1.96 \pm 0.04$. The mass-based dilute intrinsic hygroscopicity parameter $\kappa_{m,\infty} = 0.59$ corresponds to a van't Hoff factor of $J = 1.92$ (Eq. 8) and to a volume-based hygroscopicity parameter $\kappa = 1.28$ (Eq. 7, assuming volume additivity and a NaCl density of 2.165 g cm^{-3}).

The KIM two-parameter approach provides not only a good fit to the experimental data, it is also in good agreement with the much more complex multi-parameter model AIM (dashed black line). The data points in the lower left corner of Fig. 2b correspond to the co-existence of solid NaCl with an aqueous solution, which can be described by KIM Eq. (27). The water uptake observed upon hydration prior to full deliquescence is well captured by the model using the parameters obtained by the fit to the data for fully dissolved NaCl (dotted blue line; C_m , $\kappa_{m,\infty}$, and α as specified above). The water content observed upon dehydration after partial efflorescence is better matched when using the effective solubility as a free fit parameter (dotted red line). The best fit value of this “apparent solubility” $C_m^* = 0.48 \pm 0.01$ is higher than the equilibrium solubility value ($C_m = 0.36$), reflecting that aqueous solution droplets of NaCl are supersaturated at RH < 75 %. The difference between the equilibrium solubility at the deliquescence threshold and the apparent solubility at the efflorescence threshold is also illustrated in Fig. 2c, which shows the κ_m data points and model lines as a function of water activity.

4.2 Atmospheric aerosol samples

Figure 3a and b show the mass growth factors observed as a function of relative humidity upon hydration and dehydration of the atmospheric aerosol samples collected

in the tropical rainforest of Amazonia near Manaus, Brazil (AMAZE) and in the boreal forest region near St. Petersburg, Russia (SPB) as detailed in Table 2 and Sect. 3.1.

Both samples exhibit gradual and fully reversible water uptake similar to the behavior of amorphous organic substances (Mikhailov et al., 2009). The AMAZE sample is known to consist primarily of secondary organic aerosol (SOA) formed by oxidation and gas-to-particle conversion of isoprene and terpenes emitted from the rainforest ecosystem

(Chen et al., 2009; Martin et al., 2010; Pöschl et al., 2010). For the SPB sample no chemical composition data are available, but the sampling location suggests a combination of SOA from the boreal forest mixed with combustion aerosols from the urban region of St. Petersburg (Tervahattu et al., 2004; Niemi et al., 2006; Hallquist et al., 2009; Saarnio et al., 2010).

From the measurement data displayed in Figs. 3a and 3b we derived mass-based hygroscopicity parameters as outlined above, using Eq. (10) and assuming $a_w = RH/(100\%)$. The corresponding plots of κ_m vs. G_m are shown in Fig. 3c for the AMAZE sample and Fig. 3d for the SPB sample. In both cases, the observed dependence of κ_m on G_m exhibits three distinctly different sections or regimes of hygroscopicity. In the first section (quasi-eutonic regime, I) κ_m increases linearly with G_m , which can be described by Eq. (25) assuming quasi-eutonic conditions where multiple solutes co-exist in a non-aqueous state and their aqueous phase concentrations correspond to effective eutonic solubilities ($C_{m,e,i}$). In the second section (gradually deliquescent regime, II), κ_m exhibits a non-linear increase with G_m , which can be described by Eq. (22) assuming gradual dissolution of multiple water soluble compounds with different equilibrium solubilities ($C_{m,i}$). In the third section (dilute regime, III), κ_m decreases with increasing G_m and becomes concentration-independent at very high values of G_m . This behavior is analogous to the behavior observed for aqueous sodium chloride (Fig. 2b), and it can be described by Eq. (26) assuming that the water-soluble fraction of the aerosol sample is fully dissolved.

The individual physico-chemical parameters involved in Eqs. (22), (25) and (26) are not readily available for atmospheric aerosol samples consisting of multiple chemical components with unknown molecular structures and properties. Nevertheless, Eqs. (25), (22), and (26) can be re-written as follows to fit the observed dependences of κ_m on G_m in the different regimes of hygroscopicity.

Regime I (quasi – eutonic) : $\kappa_m = k_1(G_m - 1)$ (32)

Mass-based hygroscopicity parameter interaction model

E. Mikhailov et al.

[Title Page](#)

[Abstract](#)

[Introduction](#)

[Conclusions](#)

[References](#)

[Tables](#)

[Figures](#)

[◀](#)

[▶](#)

[Back](#)

[Close](#)

[Full Screen / Esc](#)

[Printer-friendly Version](#)

[Interactive Discussion](#)

Regime II (gradually deliquescent) : $\kappa_m = k_2 + k_3(G_m - 1) + k_4(G_m - 1)^{-1} + k_5(G_m - 1)^{-2}$ (33)

Regime III (dilute) : $\kappa_m = k_5(G_m - 1)^{-2} + k_6$ (34)

Here k_1 to k_6 are fit parameters related to the solubility and interaction coefficients defined in Sect. 2:

$$k_1 = \sum_{i \in \text{na}} \kappa_{m,i,\infty} C_{m,e,i} + \sum_{i \in \text{na}} C_{m,e,i}^2 \sum_{\substack{j \in \text{na} \\ j \neq i}} \alpha_{ij} C_{m,e,j} + \sum_{i \in \text{na}} \alpha_{ii} C_{m,e,i}^3 \quad (35)$$

$$k_2 = \sum_{i \in \text{na}} C_{m,i}^2 \sum_{\substack{j \in \text{aq} \\ j \neq i}} \alpha_{ij} f_j + \sum_{i \in \text{aq}} \kappa_{m,i,\infty} f_i \quad (36)$$

$$k_3 = \sum_{i \in \text{na}} \kappa_{m,i,\infty} C_{m,i} + \sum_{i \in \text{na}} C_{m,i}^2 \sum_{\substack{j \in \text{na} \\ j \neq i}} \alpha_{ij} C_{m,j} + \sum_{i \in \text{na}} \alpha_{ii} C_{m,i}^3 \quad (37)$$

$$k_4 = \sum_{i \in \text{aq}} f_i^2 \sum_{\substack{j \in \text{na} \\ j \neq i}} \alpha_{ij} C_{m,i} \quad (38)$$

$$k_5 = \sum_{i \in \text{aq}} f_i^2 \sum_{j \in \text{aq}} \alpha_{ij} f_j \quad (39)$$

$$k_6 = \sum_{i \in \text{aq}} \kappa_{m,i,\infty} f_i \quad (40)$$

The fit parameter k_5 occurs in both Eq. (33) for regime II and Eq. (34) for regime III. Note, however, that the fit parameter values of k_5 can differ between regimes II and III, because the number of species in the aqueous phase can be different upon deliquescence ($k_5(\text{II})$) and under dilute conditions ($k_5(\text{III})$). According to Eq. (17), the

Mass-based hygroscopicity parameter interaction model

E. Mikhailov et al.

[Title Page](#)

[Abstract](#)

[Introduction](#)

[Conclusions](#)

[References](#)

[Tables](#)

[Figures](#)

[◀](#)

[▶](#)

[◀](#)

[▶](#)

[Back](#)

[Close](#)

[Full Screen / Esc](#)

[Printer-friendly Version](#)

[Interactive Discussion](#)



Mass-based hygroscopicity parameter interaction model

E. Mikhailov et al.

[Title Page](#)

[Abstract](#)

[Introduction](#)

[Conclusions](#)

[References](#)

[Tables](#)

[Figures](#)

[◀](#)

[▶](#)

[◀](#)

[▶](#)

[Back](#)

[Close](#)

[Full Screen / Esc](#)

[Printer-friendly Version](#)

[Interactive Discussion](#)



fit parameter k_6 can be regarded as the dilute intrinsic hygroscopicity parameter of the investigated sample of particulate matter ($\kappa_{m,\infty}$). The other fit parameters include interaction coefficients and solubilities.

The lines in Figs. 3c and d are fits of KIM Eqs. (32)–(34) to the experimental data, and the corresponding best fit parameters $k_1 – k_6$ are listed in Table 3. The high coefficients of determination ($R^2 = 0.7 – 0.98$) confirm that the KIM approach can be used to describe the concentration dependence of the hygroscopicity of multi-component atmospheric aerosol samples. In spite of the very different origin of the two investigated atmospheric aerosol samples, most of the best fit parameter values were of a similar order of magnitude (relative deviations from ~10 % up to factor ~10). Only the fit parameter accounting for solute cross- and self-interactions under dilute conditions (k_5 (III), Eq. 39) was multiple orders of magnitude larger for the AMAZE sample than for the SPB sample.

Figures 3e and f show the hygroscopicity parameter κ_m as function of water activity. The data points were obtained by inserting the corresponding pairs of G_m and κ_m values from Fig. 3c and 3d in Eq. (10). The model lines were obtained by inserting Eqs. (32)–(34) with the fit parameters from Table 3 in Eq. (10). Again the three sections I, II, and III reflect different regimes of hygroscopicity. For the quasi-eutonic regime (I), the combination of Eqs. (10) and (32) yields a constant water activity value given by $a_w = (k_1 + 1)^{-1}$. This relation yields quasi-eutonic RH values of 64 % for the AMAZE sample and 66 % for the SPB sample (assuming $\text{RH}/(100\%) = a_w$ as justified above). At and below the quasi-eutonic RH, the observed mass growth factors are close to unity (Fig. 3a and 3b). Thus, the ±1 % uncertainty in G_m translates into ~100 % uncertainty in $G_m – 1$, which propagates further into large relative uncertainties of a_w as calculated from Eq. (10) (large horizontal error bars of the data points in the quasi-eutonic regime of Figs. 3e and f). This issue has already been discussed by Kreidenweis et al. (2008).

The gradual-deliquescent regime (II) extends up to 86 % RH for the SPB sample and even further up to 95 % RH for the AMAZE sample. Gradual deliquescence over an extended range of RH is typical for mixed multi-component particles that begin to

Mass-based hygroscopicity parameter interaction model

E. Mikhailov et al.

[Title Page](#)

[Abstract](#)

[Introduction](#)

[Conclusions](#)

[References](#)

[Tables](#)

[Figures](#)

[◀](#)

[▶](#)

[◀](#)

[▶](#)

[Back](#)

[Close](#)

[Full Screen / Esc](#)

[Printer-friendly Version](#)

[Interactive Discussion](#)



take up water vapor at a eutonic RH value and continue to grow with increasing RH up to full dissolution of all particle components (Wexler and Seinfeld 1991; Martin et al., 2000; Clegg et al., 2001; Mikhailov et al., 2009). The particularly wide range of gradual deliquescence observed for the AMAZE sample can be explained by a very small content of hygroscopic salts like ammonium sulfate and a high content of sparingly soluble secondary organic aerosol components like 2-methyltetrols from isoprene oxidation (Decesari et al., 2006).

In the dilute regime (III), the characteristic decrease of κ_m with increasing a_w is relatively steep for the AMAZE sample ($d \ln \kappa_m / d \ln a_w = 4$) and rather small for the SPB sample ($d \ln \kappa_m / d \ln a_w = 0.5$). The steep slope reflects a high value of the fit parameter k_6 , which in turn indicates strong interaction between the organic solute molecules in the AMAZE sample (Eq. 40, Table 3). The insert in Fig. 3e shows that the AMAZE particles reach a constant hygroscopicity only at RH close to 100 %. That is in contrast to the SPB sample where the concentration effect becomes negligibly small already at $RH < 99\%$ (Fig. 3f). Most likely the more prolonged concentration effect for the AMAZE particles arises from a high content of the sparingly soluble compounds (Decesari et al., 2006).

4.3 Closure between hygroscopic growth and CCN activation

In this section we test the applicability of our mass-based hygroscopicity parameter interaction model and FDHA data for closure between hygroscopic growth and CCN measurements. We used the dilute intrinsic hygroscopicity parameters obtained with KIM Eq. (34) ($\kappa_{m,\infty} = k_6$, Table 4) to predict the conditions of CCN activation. To calculate critical dry diameters of CCN activation ($D_{d,c}$) as a function of water vapor supersaturation (S_w) we inserted $\kappa_{m,\infty}$ in the simplified Köhler model (Eq. 15) using $\rho_w = 1.0 \text{ g cm}^{-3}$, $\rho_d = 2.165 \text{ g cm}^{-3}$ for NaCl and $\rho_d = (1.7 \pm 0.3) \text{ g cm}^{-3}$ for the atmospheric aerosol samples (Table 4). For the AMAZE sample an approximate average density of 1.7 g cm^{-3} was estimated based on Eq. (7) using the volume-based hygroscopicity $\kappa = 0.132$ (Gunthe et al., 2009, Table 2, CCN retrieved) and $\kappa_{m,\infty} = 0.078$

Mass-based hygroscopicity parameter interaction model

E. Mikhailov et al.

[Title Page](#)[Abstract](#)[Introduction](#)[Conclusions](#)[References](#)[Tables](#)[Figures](#)[◀](#)[▶](#)[◀](#)[▶](#)[Back](#)[Close](#)[Full Screen / Esc](#)[Printer-friendly Version](#)[Interactive Discussion](#)

(Table 4). The same density value was also used for the SPB sample.

Figure 4a shows the relationship between the critical dry diameter of CCN activation and water vapor supersaturation for NaCl particles predicted with KIM. For comparison the relationship is also calculated based on a full Köhler model (Köhler model AP3 of Rose et al., 2008) using the AIM for the parameterization of the water activity. The two model lines agree well with each other and show small differences only in the small diameter range (high supersaturation range). However, these differences are still much smaller than the differences between several experimental data obtained from direct CCN measurements (Raymond and Pandis, 2002; Giebel et al., 2002; Corrigan and Novakov, 1999; Rose et al., 2008) or derived from HTDMA measurements (Kreidenweis et al., 2005).

Figure 4b shows the relationship between the critical dry diameter of CCN activation and water vapor supersaturation for atmospheric aerosol particles predicted with KIM. For the AMAZE sample, the model predictions are in good agreement with the results of size-resolved CCN measurements (Gunthe et al., 2009) averaged over the same period as the filter sampling time (Table 2). The KIM model line falls within the error bars (standard deviations) of the experimental data points. The grey shaded area around the model line shows that uncertainties in particle density have limited influence on the prediction of critical dry diameters for CCN activation: relative variations of ρ_d by $\pm 18\%$ ($(1.7 \pm 0.3) \text{ g cm}^{-3}$) lead to relative variations of $\pm \sim 6\%$ in the critical dry diameter. For the SPB sample no CCN measurement data were available, but the lower value of $\kappa_{m,\infty}$ (-40% relative to AMAZE) implies higher critical diameter values ($+15\%$ relative to AMAZE).

Overall, Fig. 4 demonstrates that the mass-based hygroscopicity interaction model (KIM) is well-suited to link hygroscopic growth measurement data to CCN measurement data. The good agreement can be explained by the fact that the parameter value $\kappa_m = k_6$ inserted in Eq. (15) represents the intrinsic hygroscopicity $\kappa_{m,\infty}$, which captures the characteristics of water uptake by dilute solution droplets as formed upon CCN activation.

5 Summary and conclusions

In this manuscript, we present a mass-based model approach for efficient description of concentration-dependent water uptake by atmospheric aerosol particles. Equations (6)–(10) define the mass-based hygroscopicity parameter κ_m , which is equivalent to the volume-based hygroscopicity parameter introduced by Petters and Kreidenweis (2007) but independent of deviations from volume additivity. Equations (12)–(15) describe a simple Köhler model in which κ_m can be used to predict the particle critical diameter for activation to a cloud droplet.

In Eqs. (16)–(24) we develop a κ_m -interaction model (KIM) that combines a dilute intrinsic hygroscopicity parameter with additional self- and cross-interaction parameters describing non-ideal solution behavior and concentration dependencies of single- and multi-component systems. For specific conditions, the main model equation (Eq. 22) can be reduced to simplified versions (Eqs. 25–28).

By application of KIM to water uptake measurement data of atmospheric aerosol samples, we can distinguish three different regimes of hygroscopicity: (I) A quasi-eutonic regime at low-humidity ($\lesssim 60\% \text{ RH}$) where the solutes co-exist in aqueous and non-aqueous phase (Eq. 32); (II) a gradually deliquescent regime at intermediate humidity ($\sim 60\% \text{--} 90\% \text{ RH}$) where different solutes undergo gradual dissolution in the aqueous phase (Eq. 33); and (III) a dilute regime at high humidity ($\gtrsim 90\% \text{ RH}$) where the solutes are fully dissolved approaching their dilute intrinsic hygroscopicity (Eq. 34).

In each of these regimes, the concentration dependence of κ_m can be described by simplified model equations (Eqs. 32–34) based on observable mass growth factors and a series of fit parameters ($k_1 \text{--} k_6$) summarizing the combined effects of the dilute intrinsic hygroscopicity and interaction parameters of all involved chemical components. The parameter k_6 determined by fitting of Eq. (34) to hygroscopic growth data obtained in the dilute regime at high humidity represents the dilute intrinsic hygroscopicity of the aerosol ($\kappa_{m,\infty}$) and can be used to predict CCN activation diameters as a function of water vapor supersaturation. For sodium chloride reference particles as well

Mass-based hygroscopicity parameter interaction model

E. Mikhailov et al.

[Title Page](#)

[Abstract](#)

[Introduction](#)

[Conclusions](#)

[References](#)

[Tables](#)

[Figures](#)

◀

▶

[Back](#)

[Close](#)

[Full Screen / Esc](#)

[Printer-friendly Version](#)

[Interactive Discussion](#)



Mass-based hygroscopicity parameter interaction model

E. Mikhailov et al.

[Title Page](#)[Abstract](#)[Introduction](#)[Conclusions](#)[References](#)[Tables](#)[Figures](#)[◀](#)[▶](#)[◀](#)[▶](#)[Back](#)[Close](#)[Full Screen / Esc](#)[Printer-friendly Version](#)[Interactive Discussion](#)

as for pristine rainforest aerosols consisting mostly of secondary organic matter, we obtained good agreement between the predicted and measured critical diameters of CCN activation.

The good agreement between size-resolved CCN measurements and filter-based mass growth factor measurements is consistent with the fairly homogeneous and hardly size-dependent chemical composition of the pristine rainforest aerosols.

For aerosols that are externally mixed and exhibit a strong size dependence of particle hygroscopicity (e.g., in polluted megacity air, Rose et al., 2010, 2011; Gunthe et al. 2011), it may be useful to perform size-resolved measurements of mass growth factors 10 using multi-stage impactor samples. Moreover, it may be useful to combine the KIM approach with hygroscopicity distribution concepts that resolve the size-dependence of the hygroscopic growth and CCN activity of aerosol particles (e.g., Su et al., 2010; Cerully et al., 2011). For detailed understanding and efficient description of aerosol-water interactions, we suggest and intend to pursue further investigations along these 15 lines.

Acknowledgements. This work has been supported by the Max Planck Society (MPG), the Russian Foundation for Basic Research (grant 09-05-00883-a), the German Research Foundation (DFG-SPP 1294-HALO, grant PO 1013/2), and the European Commission under the integrated projects EUCAARI (grant 036833-2) and PEGASOS (grant 265148). The 20 authors thank M. O. Andreae, P. Artaxo, S. T. Martin, S. S. Gunthe, and the entire AMAZE-08 team for support, and H. Su for helpful comments.

The service charges for this open access publication have been covered by the Max Planck Society.

25 References

Bilde, M. and Svenningsson, B.: CCN activation of slightly soluble organics: the importance of small amounts of inorganic salt and particle phase, Tellus B, 56, 128–134, 2004.

Mass-based hygroscopicity parameter interaction model

E. Mikhailov et al.

[Title Page](#)

[Abstract](#)

[Introduction](#)

[Conclusions](#)

[References](#)

[Tables](#)

[Figures](#)

◀

▶

◀

▶

[Back](#)

[Close](#)

[Full Screen / Esc](#)

[Printer-friendly Version](#)

[Interactive Discussion](#)



Carrico, C. M., Petters, M. D., Kreidenweis, S. M., Sullivan, A. P., McMeeking, G. R., Levin, E. J. T., Engling, G., Malm, W. C., and Collett Jr., J. L.: Water uptake and chemical composition of fresh aerosols generated in open burning of biomass, *Atmos. Chem. Phys.*, 10, 5165–5178, doi:10.5194/acp-10-5165-2010, 2010.

5 Cerully, K. M., Raatikainen, T., Lance, S., Tkacik, D., Tiitta, P., Petäjä, T., Ehn, M., Kulmala, M., Worsnop, D. R., Laaksonen, A., Smith, J. N., and Nenes, A.: Aerosol hygroscopicity and CCN activation kinetics in a boreal forest environment during the 2007 EUCAARI campaign, *Atmos. Chem. Phys. Discuss.*, 11, 15029–15074, doi:10.5194/acpd-11-15029-2011, 2011.

10 Chen, Q., Farmer, D. K., Schneider, J., Zorn, S. R., Heald, C. L., Karl, T. G., Guenther, A., Allan, J. D., Robinson, N., Coe, H., Kimmel, J. R., Pauliquevis, T., Borrmann, S., Pöschl, U., Andreae, M. O., Artaxo, P., Jimenez, J. L., and Martin, S. T.: Mass spectral characterization of submicron biogenic organic particles in the Amazon Basin, *Geophys. Res. Lett.*, 36, L20806, doi:10.1029/2009GL039880, 2009.

15 Clarke, E. C. W. and Glew, D. N.: Evaluation of the thermodynamic functions for aqueous sodium chloride from equilibrium and calorimetric measurements below 154 °C, *J. Phys. Chem. Ref. Data*, 14, 489–609, 1985.

Clegg, S. L. and Seinfeld, J. H.: Thermodynamic models of aqueous solutions containing inorganic electrolytes and dicarboxylic acids at 298.15 K. I. The acids as non-dissociating components, *J. Phys. Chem. A*, 110, 5692–5717, doi:10.1021/jp056149k, 2006a.

20 Clegg, S. L. and Seinfeld, J. H.: Thermodynamic models of aqueous solutions containing inorganic electrolytes and dicarboxylic acids at 298.15 K. II. Systems including dissociation equilibria, *J. Phys. Chem. A*, 110, 5718–5734, doi:10.1021/jp056150j, 2006b.

Clegg, S. L., Brimblecombe, P., and Wexler, A. S.: A thermodynamic model of the system $\text{H}^+ \text{-NH}_4^+ \text{-Na}^+ \text{-SO}_4^{2-} \text{-NO}_3^- \text{-Cl}^- \text{-H}_2\text{O}$ at 298.15 K, *J. Phys. Chem. A*, 102, 2155–2171, 1998.

25 Clegg, S. L., Seinfeld, J. H., and Brimblecombe, P.: Thermodynamic modelling of aqueous aerosols containing electrolytes and dissolved organic compounds, *Aerosol Sci.*, 32, 6, 713–738, doi:10.1016/S0021-8502(00)00105-1, 2001.

Colberg, C. A., Krieger, U. K., and Peter, T.: Morphological investigations of single levitated $\text{H}_2\text{SO}_4/\text{NH}_3/\text{H}_2\text{O}$ aerosol particles during deliquescence/efflorescence experiments, *J. Phys. Chem. A*, 108, 2700–2709, doi:10.1021/jp037628r, 2004.

30 Corrigan, C. E. and Novakov, T.: Cloud condensation nucleus activity of organic compounds: a laboratory study, *Atmos. Environ.*, 33, 17, 2661–2668, doi:10.1016/S1352-2310(98)00310-0, 1999.

**Mass-based
hygroscopicity
parameter interaction
model**

E. Mikhailov et al.

[Title Page](#)[Abstract](#)[Introduction](#)[Conclusions](#)[References](#)[Tables](#)[Figures](#)[Back](#)[Close](#)[Full Screen / Esc](#)[Printer-friendly Version](#)[Interactive Discussion](#)

Decesari, S., Fuzzi, S., Facchini, M. C., Mircea, M., Emblico, L., Cavalli, F., Maenhaut, W., Chi, X., Schkolnik, G., Falkovich, A., Rudich, Y., Claeys, M., Pashynska, V., Vas, G., Kourtchev, I., Vermeylen, R., Hoffer, A., Andreae, M. O., Tagliavini, E., Moretti, F., and Artaxo, P.: Characterization of the organic composition of aerosols from Rondônia, Brazil, during the LBA-SMOCC 2002 experiment and its representation through model compounds, *Atmos. Chem. Phys.*, 6, 375–402, doi:10.5194/acp-6-375-2006, 2006.

Duplissy, J., DeCarlo, P. F., Dommen, J., Alfarra, M. R., Metzger, A., Barmpadimos, I., Prevot, A. S. H., Weingartner, E., Tritscher, T., Gysel, M., Aiken, A. C., Jimenez, J. L., Canagaratna, M. R., Worsnop, D. R., Collins, D. R., Tomlinson, J., and Baltensperger, U.: Relating hygroscopicity and composition of organic aerosol particulate matter, *Atmos. Chem. Phys.*, 11, 1155–1165, doi:10.5194/acp-11-1155-2011, 2011.

Finlayson-Pitts, B. J. and Pitts, J. N.: Chemistry of the upper and lower atmosphere: Theory, experiments and applications, Academic Press, San Diego, CA, 969 pp., 2000.

Fitzgerald, J. W.: Dependence of supersaturation spectrum of CCN on aerosol size distribution and composition, *J. Atmos. Sci.*, 30, 628–634, 1973.

Flatau, P. J., Walko, R. L., and Cotton, W. R.: Polynomial fits to saturation vapor pressure, *J. Appl. Meteorol.*, 31, 12, 1507–1513, 1992.

Fors, E. O., Swietlicki, E., Svenssonsson, B., Kristensson, A., Frank, G. P., and Sporre, M.: Hygroscopic properties of the ambient aerosol in southern Sweden – a two year study, *Atmos. Chem. Phys.*, 11, 8343–8361, doi:10.5194/acp-11-8343-2011, 2011.

Fountoukis, C. and Nenes, A.: ISORROPIA II: a computationally efficient thermodynamic equilibrium model for K^+ – Ca^{2+} – Mg^{2+} – NH_4^+ – Na^+ – SO_4^{2-} – NO_3^- – Cl^- – H_2O aerosols, *Atmos. Chem. Phys.*, 7, 4639–4659, doi:10.5194/acp-7-4639-2007, 2007.

Fredenslund, A., Jones, R. L., and Prausnitz, J. M.: Group-contribution estimation of activity coefficients in nonideal liquid mixtures, *AIChE J.*, 21, 6, 1086–1099, 1975.

Giebl, H., Berner, A., Reischl, G., Puxbaum, H., Kasper-Giebl, A., and Hitzenberger, R.: CCN activation of oxalic and malonic acid test aerosols with the University of Vienna cloud condensation nuclei counter, *J. Aerosol Sci.*, 33, 12, 1623–1634, doi:10.1016/S0021-8502(02)00115-5, 2002.

Good, N., Topping, D. O., Allan, J. D., Flynn, M., Fuentes, E., Irwin, M., Williams, P. I., Coe, H., and McFiggans, G.: Consistency between parameterisations of aerosol hygroscopicity and CCN activity during the RHAMBLe discovery cruise, *Atmos. Chem. Phys.*, 10, 3189–3203, doi:10.5194/acp-10-3189-2010, 2010b.

- Good, N., Topping, D. O., Duplissy, J., Gysel, M., Meyer, N. K., Metzger, A., Turner, S. F., Baltensperger, U., Ristovski, Z., Weingartner, E., Coe, H., and McFiggans, G.: Widening the gap between measurement and modelling of secondary organic aerosol properties?, *Atmos. Chem. Phys.*, 10, 2577–2593, doi:10.5194/acp-10-2577-2010, 2010a.
- 5 Gunthe, S. S., King, S. M., Rose, D., Chen, Q., Roldin, P., Farmer, D. K., Jimenez, J. L., Artaxo, P., Andreae, M. O., Martin, S. T., and Pöschl, U.: Cloud condensation nuclei in pristine tropical rainforest air of Amazonia: size-resolved measurements and modeling of atmospheric aerosol composition and CCN activity, *Atmos. Chem. Phys.*, 9, 7551–7575, doi:10.5194/acp-9-7551-2009, 2009.
- 10 Gunthe, S. S., Rose, D., Su, H., Garland, R. M., Achtert, P., Nowak, A., Wiedensohler, A., Kuwata, M., Takegawa, N., Kondo, Y., Hu, M., Shao, M., Zhu, T., Andreae, M. O., and Pöschl, U.: Cloud condensation nuclei (CCN) from fresh and aged air pollution in the megacity region of Beijing, *Atmos. Chem. Phys.*, 11, 11023–11039, doi:10.5194/acp-11-11023-2011, 2011.
- 15 Gysel, M., Weingartner, E., Nyeki, S., Paulsen, D., Baltensperger, U., Galambos, I., and Kiss, G.: Hygroscopic properties of water-soluble matter and humic-like organics in atmospheric fine aerosol, *Atmos. Chem. Phys.*, 4, 35–50, doi:10.5194/acp-4-35-2004, 2004.
- Gysel, M., Weingartner, E., and Baltensperger, U.: Hygroscopicity of aerosol particles at low temperatures. 2. Theoretical and experimental hygroscopic properties of laboratory generated aerosols, *Environ. Sci. Technol.*, 36, 63–68, doi:10.1021/es010055g, 2002.
- 20 Hallquist, M., Wenger, J. C., Baltensperger, U., Rudich, Y., Simpson, D., Claeys, M., Dommen, J., Donahue, N. M., George, C., Goldstein, A. H., Hamilton, J. F., Herrmann, H., Hoffmann, T., Inuma, Y., Jang, M., Jenkin, M. E., Jimenez, J. L., Kiendler-Scharr, A., Maenhaut, W., McFiggans, G., Mentel, Th. F., Monod, A., Prévôt, A. S. H., Seinfeld, J. H., Surratt, J. D., Szmigielski, R., and Wildt, J.: The formation, properties and impact of secondary organic aerosol: current and emerging issues, *Atmos. Chem. Phys.*, 9, 5155–5236, doi:10.5194/acp-9-5155-2009, 2009.
- 25 Huff Hartz, K. E., Rosenørn, T., Ferchak, S. R., Raymond, T. M., Bilde, M., Donahue, N. M., and Pandis, S. N.: Cloud condensation nuclei activation of monoterpane and sesquiterpene secondary organic aerosol, *J. Geophys. Res.*, 110, D14208, doi:10.1029/2004JD005754, 2005.
- 30 Irwin, M., Good, N., Crosier, J., Choularton, T. W., and McFiggans, G.: Reconciliation of measurements of hygroscopic growth and critical supersaturation of aerosol particles in central Germany, *Atmos. Chem. Phys.*, 10, 11737–11752, doi:10.5194/acp-10-11737-2010, 2010.

Mass-based hygroscopicity parameter interaction model

E. Mikhailov et al.

[Title Page](#)

[Abstract](#)

[Introduction](#)

[Conclusions](#)

[References](#)

[Tables](#)

[Figures](#)



[Back](#)

[Close](#)

[Full Screen / Esc](#)

[Printer-friendly Version](#)

[Interactive Discussion](#)



- Junge, C. and McLaren, E.: Relationship of cloud nuclei spectra to aerosol size distribution and composition, *J. Atmos. Sci.*, 28, 382–390, 1971.
- Krämer, L., Pöschl, U., and Niessner, R.: Microstructural rearrangement of sodium chloride condensation aerosol particles on interaction with water vapor, *J. Aerosol. Sci.*, 31, 6, 673–685, doi:10.1016/S0021-8502(99)00551-0, 2000.
- Kreidenweis, S. M., Koehler, K., DeMott, P. J., Prenni, A. J., Carrico, C., and Ervens, B.: Water activity and activation diameters from hygroscopicity data – Part I: Theory and application to inorganic salts, *Atmos. Chem. Phys.*, 5, 1357–1370, doi:10.5194/acp-5-1357-2005, 2005.
- Kreidenweis, S. M., Petters, M. D., and DeMott, P. J.: Single-parameter estimates of aerosol water content, *Environ. Res. Lett.*, 3, 035002, doi:10.1088/1748-9326/3/3/035002, 2008.
- Kulmala, M., Laaksonen, A., Charlson, R. J., and Korhonen, P.: Clouds without supersaturation, *Nature*, 388, 336–337, 1997.
- Laaksonen, A., Korhonen, P., Kulmala, M., and Charlson, R. J.: Modification of the Köhler equation to include soluble trace gases and slightly soluble substances, *J. Atmos. Sci.*, 55, 853–862, 1998.
- Marcolli, C., and Krieger, U. K.: Phase changes during hygroscopic cycles of mixed organic/inorganic model systems of tropospheric aerosols, *J. Phys. Chem. A.*, 110, 1881–1893, doi:10.1021/jp0556759, 2006.
- Marcolli, C., Luo, B., and Peter, T.: Mixing of the organic aerosol fractions: Liquids as the thermodynamically stable phases, *J. Phys. Chem. A.*, 108, 2216–2224, doi:10.1021/jp036080l, 2004.
- Martin, S. T.: Phase transitions of aqueous atmospheric particles, *Chem. Rev.*, 100, 9, 3403–3453, doi:10.1021/cr990034t, 2000.
- Martin, S. T., Andreae, M. O., Althausen, D., Artaxo, P., Baars, H., Borrmann, S., Chen, Q., Farmer, D. K., Guenther, A., Gunthe, S. S., Jimenez, J. L., Karl, T., Longo, K., Manzi, A., Müller, T., Pauliquevis, T., Petters, M. D., Prenni, A. J., Pöschl, U., Rizzo, L. V., Schneider, J., Smith, J. N., Swietlicki, E., Tota, J., Wang, J., Wiedensohler, A., and Zorn, S. R.: An overview of the Amazonian Aerosol Characterization Experiment 2008 (AMAZE-08), *Atmos. Chem. Phys.*, 10, 11415–11438, doi:10.5194/acp-10-11415-2010, 2010.
- Metzger, S., Steil, B., Xu, L., Penner, J. E., and Lelieveld, J.: Aerosol hygroscopic growth parameterization based on a solute specific coefficient, *Atmos. Chem. Phys. Discuss.*, 11, 24813–24855, doi:10.5194/acpd-11-24813-2011, 2011.
- Mifflin, A. L., Smith, M. L., and Martin, S. T.: Morphology hypothesized to influence aerosol par-

Mass-based hygroscopicity parameter interaction model

E. Mikhailov et al.

[Title Page](#)

[Abstract](#)

[Introduction](#)

[Conclusions](#)

[References](#)

[Tables](#)

[Figures](#)



[Back](#)

[Close](#)

[Full Screen / Esc](#)

[Printer-friendly Version](#)

[Interactive Discussion](#)



Mass-based hygroscopicity parameter interaction model

E. Mikhailov et al.

[Title Page](#)[Abstract](#)[Introduction](#)[Conclusions](#)[References](#)[Tables](#)[Figures](#)[◀](#)[▶](#)[Back](#)[Close](#)[Full Screen / Esc](#)[Printer-friendly Version](#)[Interactive Discussion](#)

ticle deliquescence, *Phys. Chem. Chem. Phys.*, 11, 10095–10107, doi:10.1039/B910432A 2009.

Mikhailov, E., Vlasenko, S., Niessner, R., and Pöschl, U.: Interaction of aerosol particles composed of protein and salts with water vapor: hygroscopic growth and microstructural rearrangement, *Atmos. Chem. Phys.*, 4, 323–350, doi:10.5194/acp-4-323-2004, 2004.

Mikhailov, E., Vlasenko, S., Martin, S. T., Koop, T., and Pöschl, U.: Amorphous and crystalline aerosol particles interacting with water vapor: conceptual framework and experimental evidence for restructuring, phase transitions and kinetic limitations, *Atmos. Chem. Phys.*, 9, 9491–9522, doi:10.5194/acp-9-9491-2009, 2009.

10 Mikhailov, E. F., Merkulov, V. V., Vlasenko, S. S., and Pöschl, U.: Filter-based differential hygroscopicity analyzer of aerosol particles, *Izv. Atmos. Oceanic Phys.*, in press, 47, 6, 747–759, 2011.

Mochida, M., Kuwata, M., Miyakawa, T., Takegawa, N., Kawamura, K., and Kondo, Y.: Relationship between hygroscopicity and cloud condensation nuclei activity for urban aerosols in Tokyo, *J. Geophys. Res.*, 111, D23204, doi:10.1029/2005JD006980, 2006.

Niemi, J. V., Saarikoski, S., Tervahattu, H., Mäkelä, T., Hillamo, R., Vehkamäki, H., Sogacheva, L., and Kulmala, M.: Changes in background aerosol composition in Finland during polluted and clean periods studied by TEM/EDX individual particle analysis, *Atmos. Chem. Phys.*, 6, 5049–5066, doi:10.5194/acp-6-5049-2006, 2006.

20 Petters, M. D. and Kreidenweis, S. M.: A single parameter representation of hygroscopic growth and cloud condensation nucleus activity, *Atmos. Chem. Phys.*, 7, 1961–1971, doi:10.5194/acp-7-1961-2007, 2007.

Petters, M. D. and Kreidenweis, S. M.: A single parameter representation of hygroscopic growth and cloud condensation nucleus activity – Part 2: Including solubility, *Atmos. Chem. Phys.*, 8, 6273–6279, doi:10.5194/acp-8-6273-2008, 2008.

Petters, M. D., Carrico, C. M., Kreidenweis, S. M., Prenni, A. J., DeMott, P. J., Collett, J. L., and Moosmüller, H.: Cloud condensation nucleation activity of biomass burning aerosol, *J. Geophys. Res.*, 114, D22205, doi:10.1029/2009JD012353, 2009.

30 Pöschl, U., Martin, S. T., Sinha, B., Chen, Q., Gunthe, S. S., Huffman, J. A., Borrmann, S., Farmer, D. K., Garland, R. M., Helas, G., Jimenez, J.L., King, S. M., Manzi, A., Mikhailov, E., Pauliquevis, T., Petters, M. D., Prenni, A. J., Roldin, P., Rose, D., Schneider, J., Su, H., Zorn, S. R., Artaxo, P., Andreae, M. O.: Rainforest Aerosols as Biogenic Nuclei of Clouds and Precipitation in the Amazon, *Science*, 329, 5998, 1513–1516, doi:10.1126/science.1191056,

2010.

- Pringle, K. J., Tost, H., Pozzer, A., Pöschl, U., and Lelieveld, J.: Global distribution of the effective aerosol hygroscopicity parameter for CCN activation, *Atmos. Chem. Phys.*, 10, 5241–5255, doi:10.5194/acp-10-5241-2010, 2010.
- Pruppacher, H. R. and Klett, J. D.: *Microphysics of clouds and precipitation*, Kluwer Academic Publishers, Dordrecht, The Netherlands, 2000.
- Raymond T. M. and Pandis S. N.: Cloud activation of single-component organic aerosol particles, *J. Geophys. Res.*, 107, 4787, doi:10.1029/2002JD002159, 2002.
- Raymond, T. M. and Pandis, S. N.: Formation of cloud droplets by multicomponent organic particles, *J. Geophys. Res.*, 108, 4469, doi:10.1029/2003JD003503, 2003.
- Rissler, J., Swietlicki, E., Zhou, J., Roberts, G., Andreae, M. O., Gatti, L. V., and Artaxo, P.: Physical properties of the sub-micrometer aerosol over the Amazon rain forest during the wet-to-dry season transition - comparison of modeled and measured CCN concentrations, *Atmos. Chem. Phys.*, 4, 2119–2143, doi:10.5194/acp-4-2119-2004, 2004.
- Roberts, G. C., Day, D. A., Russell, L. M., Dunlea, E. J., Jimenez, J. L., Tomlinson, J. M., Collins, D. R., Shinozuka, Y., and Clarke, A. D.: Characterization of particle cloud droplet activity and composition in the free troposphere and the boundary layer during INTEX-B, *Atmos. Chem. Phys.*, 10, 6627–6644, doi:10.5194/acp-10-6627-2010, 2010.
- Rose, D., Gunthe, S. S., Mikhailov, E., Frank, G. P., Dusek, U., Andreae, M. O., and Pöschl, U.: Calibration and measurement uncertainties of a continuous-flow cloud condensation nuclei counter (DMT-CCNC): CCN activation of ammonium sulfate and sodium chloride aerosol particles in theory and experiment, *Atmos. Chem. Phys.*, 8, 1153–1179, doi:10.5194/acp-8-1153-2008, 2008.
- Rose, D., Nowak, A., Achtert, P., Wiedensohler, A., Hu, M., Shao, M., Zhang, Y., Andreae, M. O., and Pöschl, U.: Cloud condensation nuclei in polluted air and biomass burning smoke near the mega-city Guangzhou, China – Part 1: Size-resolved measurements and implications for the modeling of aerosol particle hygroscopicity and CCN activity, *Atmos. Chem. Phys.*, 10, 3365–3383, doi:10.5194/acp-10-3365-2010, 2010.
- Rose, D., Gunthe, S. S., Su, H., Garland, R. M., Yang, H., Berghof, M., Cheng, Y. F., Wehner, B., Achtert, P., Nowak, A., Wiedensohler, A., Takegawa, N., Kondo, Y., Hu, M., Zhang, Y., Andreae, M. O., and Pöschl, U.: Cloud condensation nuclei in polluted air and biomass burning smoke near the mega-city Guangzhou, China – Part 2: Size-resolved aerosol chemical composition, diurnal cycles, and externally mixed weakly CCN-active soot particles, *Atmos.*

Mass-based
hygroscopicity
parameter interaction
model

E. Mikhailov et al.

[Title Page](#)

[Abstract](#)

[Introduction](#)

[Conclusions](#)

[References](#)

[Tables](#)

[Figures](#)



[Back](#)

[Close](#)

[Full Screen / Esc](#)

[Printer-friendly Version](#)

[Interactive Discussion](#)



- Ruehl, C. R., Chuang, P. Y., and Nenes, A.: Aerosol hygroscopicity at high (99 to 100%) relative humidities, *Atmos. Chem. Phys.*, 10, 1329–1344, doi:10.5194/acp-10-1329-2010, 2010.
- Saarnio, K., Aurela, M., Timonen, H., Saarikoski, S., Teinilä, K., Mäkelä, T., Sofiev, M., Koskinen, J., Aalto, P. P., Kulmala, M., Kukkonen, J., and Hillamo, R.: Chemical composition of fine particles in fresh smoke plumes from boreal wild-land fires in Europe, *Sci. Total Environ.*, 408, 12, 2527–2542, doi:10.1016/j.scitotenv.2010.03.010, 2010.
- Seinfeld, J. H. and Pandis, S. N.: *Atmospheric Chemistry and Physics: From Air Pollution to Climate Change*, John Wiley and Sons, Inc., New York, USA, 2006.
- Setschenov, J.: Über die Konstitution der Salzlösungen aufgrund ihres Verhaltens zu Kohlensäure, *Z. Phys. Chem.*, 4, 117–125, 1889.
- Shulman, M. L., Jacobson, M. C., Carlson, R. J., Synovec, R. E., and Young, T. E.: Dissolution behavior and surface tension effects of organic compounds in nucleating cloud droplets, *Geophys. Res. Lett.*, 23, 3, 277–280, doi:10.1029/95GL03810, 1996.
- Smith, M. L., Kuwata, M., and Martin S. T.: Secondary organic material produced by the dark ozonolysis of α -pinene minimally affects the deliquescence and efflorescence of ammonium sulfate, *Aerosol Sci. Technol.*, 45, 244–261, doi:10.1080/02786826.2010.532178, 2011.
- Sjogren, S., Gysel, M., Weingartner, E., Baltensperger, U., Cubison, M. J., Coe, H., Zardini, A. A., Marcolli, C., Krieger, U. R., and Peter, T.: Hygroscopic growth and water uptake kinetics of two-phase aerosol particles consisting of ammonium sulphate, adipic and humic acid mixtures, *J. Aerosol Sci.*, 38, 157–171, 2007.
- Stephen, H. and Stephen, T. (Eds.): *Solubilities of inorganic and organic compounds*, Pergamon Press, Oxford, UK, 1963.
- Stokes, R. H. and Robinson, R. A.: Interactions in aqueous nonelectrolyte solutions: I. Solute-solvent equilibria, *J. Phys. Chem.* 70, 2126–2130, 1966.
- Su, H., Rose, D., Cheng, Y. F., Gunthe, S. S., Massling, A., Stock, M., Wiedensohler, A., Andreae, M. O., and Pöschl, U.: Hygroscopicity distribution concept for measurement data analysis and modeling of aerosol particle mixing state with regard to hygroscopic growth and CCN activation, *Atmos. Chem. Phys.*, 10, 7489–7503, doi:10.5194/acp-10-7489-2010, 2010.
- Sullivan, R. C., Moore, M. J. K., Petters, M. D., Kreidenweis, S. M., Roberts, G. C., and Prather, K. A.: Effect of chemical mixing state on the hygroscopicity and cloud nucleation properties of calcium mineral dust particles, *Atmos. Chem. Phys.*, 9, 3303–3316, doi:10.5194/acp-9-

Mass-based hygroscopicity parameter interaction model

E. Mikhailov et al.

[Title Page](#)

[Abstract](#)

[Introduction](#)

[Conclusions](#)

[References](#)

[Tables](#)

[Figures](#)



[Full Screen / Esc](#)

[Printer-friendly Version](#)

[Interactive Discussion](#)



5

Svenningsson, B., Rissler, J., Swietlicki, E., Mircea, M., Bilde, M., Facchini, M. C., Decesari, S., Fuzzi, S., Zhou, J., Mørnster, J., and Rosenørn, T.: Hygroscopic growth and critical supersaturations for mixed aerosol particles of inorganic and organic compounds of atmospheric relevance, *Atmos. Chem. Phys.*, 6, 1937–1952, doi:10.5194/acp-6-1937-2006, 2006.

10

Tang, I. N. and Munkelwitz, H. R.: Composition and temperature dependence of the deliquescence properties of hygroscopic aerosol, *Atmos. Environ.*, 27A, 4, 467–473, doi:10.1016/0960-1686(93)90204-C, 1993.

10

Tervahattu, H., Hongisto, M., Aarnio, P., Kupiainen, K., and Sillanpää, M.: Composition and origins of aerosol during a high PM₁₀ episode in Finland, *Boreal Environ. Res.*, 9, 335–345, 2004.

15

Topping, D. O., McFiggans, G. B., and Coe, H.: A curved multi-component aerosol hygroscopicity model framework: Part 1 - Inorganic compounds, *Atmos. Chem. Phys.*, 5, 1205–1222, doi:10.5194/acp-5-1205-2005, 2005.

20

Wang, Z., King, S. M., Freney, E., Rosenoern, T., Smith, M. L., Chen, Q., Kuwata, M., Lewis, E. R., Pöschl, U., Wang, W., Buseck, P. R., and Martin, S. T.: The Dynamic Shape Factor of Sodium Chloride Nanoparticles as Regulated by Drying Rate, *Aerosol Sci. Technol.*, 44, 11, 939–953, doi:10.1080/02786826.2010.503204, 2010.

25

Wex, H., Stratmann, F., Hennig, T., Hartmann, S., Niedermeier, D., Nilsson, E., Ocskay, R., Rose, D., Salma, I., and Ziese, M.: Connecting hygroscopic growth at high humidities to cloud activation for different particle types, *Environ. Res. Lett.*, 3, 035004, doi:10.1088/1748-9326/3/3/035004, 2008.

30

Wexler, A. S. and Seinfeld, J. H.: Second-generation inorganic aerosol model, *Atmos. Environ.*, 25A, 12, 2731–2748, doi:10.1016/0960-1686(91)90203-J, 1991.

35

Wexler, A. S. and Clegg, S. L.: Atmospheric aerosol models for systems including the ions H⁺, NH₄⁺, Na⁺, SO₄²⁻, NO₃⁻, Cl⁻, Br⁻, and H₂O, *J. Geophys. Res.*, 107, D14, 4207, doi:10.1029/2001JD000451, 2002.

40

Zardini, A. A., Sjogren, S., Marcolli, C., Krieger, U. K., Gysel, M., Weingartner, E., Baltensperger, U., and Peter, T.: A combined particle trap/HTDMA hygroscopicity study of mixed inorganic/organic aerosol particles, *Atmos. Chem. Phys.*, 8, 5589–5601, doi:10.5194/acp-8-5589-2008, 2008.

Zuend, A., Marcolli, C., Booth, A. M., Lienhard, D. M., Soonsin, V., Krieger, U. K., Topping, D. O., McFiggans, G., Peter, T., and Seinfeld, J. H.: New and extended parameterization of

Mass-based hygroscopicity parameter interaction model

E. Mikhailov et al.

[Title Page](#)

[Abstract](#)

[Introduction](#)

[Conclusions](#)

[References](#)

[Tables](#)

[Figures](#)

◀

▶

◀

▶

[Back](#)

[Close](#)

[Full Screen / Esc](#)

[Printer-friendly Version](#)

[Interactive Discussion](#)



the thermodynamic model AIOMFAC: calculation of activity coefficients for organic-inorganic mixtures containing carboxyl, hydroxyl, carbonyl, ether, ester, alkenyl, alkyl, and aromatic functional groups, *Atmos. Chem. Phys.*, 11, 9155–9206, doi:10.5194/acp-11-9155-2011, 2011.

ACPD

11, 30877–30918, 2011

Mass-based
hygroscopicity
parameter interaction
model

E. Mikhailov et al.

Title Page	
Abstract	Introduction
Conclusions	References
Tables	Figures
◀	▶
◀	▶
Back	Close
Full Screen / Esc	
Printer-friendly Version	
Interactive Discussion	

Mass-based hygroscopicity parameter interaction model

E. Mikhailov et al.

[Title Page](#)

[Abstract](#)

[Introduction](#)

[Conclusions](#)

[References](#)

[Tables](#)

[Figures](#)

[◀](#)

[▶](#)

[◀](#)

[▶](#)

[Back](#)

[Close](#)

[Full Screen / Esc](#)

[Printer-friendly Version](#)

[Interactive Discussion](#)

Symbol	SI-unit	Quantity
a_w		water activity
C_m	kg kg^{-1}	solubility of the solute in water
$C_{m,e}$	kg kg^{-1}	eutonic solubility
$c_{m,i}$	kg kg^{-1}	mass concentration of individual component in solution
D	m	diameter of a spherical aqueous droplet
D_d	m	diameter of the dry aerosol particle
$D_{d,c}$	m	critical dry diameter
f_i		mass fraction of individual component of particulate matter
G_D		diameter growth factor
G_m		mass growth factor
J		van't Hoff factor
m_d	kg	mass of the dry particle in the aqueous droplet
M_w	kg mol^{-1}	molar mass of pure water
m_w	kg	mass of the water in the aqueous droplet
R	$\text{J K}^{-1} \text{mol}^{-1}$	universal gas constant
RH	%	relative humidity
S_w		water vapor saturation ratio
S_w	%	water vapor supersaturation
$S_{w,c}$		critical water vapor saturation ratio
T	K	temperature
α_{ij}, α_{ii}		cross-, self-interaction coefficient
κ		volume-based hygroscopicity parameter
K_m		mass-based hygroscopicity parameter
$K_{m,i,\infty}$		mass-based dilute intrinsic hygroscopicity
μ	mol kg^{-1}	molality
ρ	kg m^{-3}	density of the aqueous solution droplet
ρ_d	kg m^{-3}	density of the dry particle material
ρ_w	kg m^{-3}	density of pure water
σ	J m^{-2}	surface tension of solution droplet
σ_w	J m^{-2}	surface tension of pure water

**Mass-based
hygroscopicity
parameter interaction
model**

E. Mikhailov et al.

Table 2. Atmospheric aerosol sampling location and parameters.

Sample ID	Sampling location	Sampling level above surface, m	Sampling period	Aerosol mass used for FDHA analysis, mg
AMAZE	Manaus, Brazil 02°35' S, 60°12' W	39	15–20 February 2008	0.061±0.002
SPB	Saint-Petersburg, Russia 59°88' N, 29°82' E	15	18–27 May 2009	0.60±0.01

[Title Page](#)
[Abstract](#) [Introduction](#)
[Conclusions](#) [References](#)
[Tables](#) [Figures](#)
[◀](#) [▶](#)
[◀](#) [▶](#)
[Back](#) [Close](#)
[Full Screen / Esc](#)

[Printer-friendly Version](#)
[Interactive Discussion](#)



Mass-based hygroscopicity parameter interaction model

E. Mikhailov et al.

Table 3. Best fit parameters ($k_1 - k_6$) obtained with KIM Eqs. (35)–(40) and eutonic relative humidity, RH_e obtained for Amazon (AMAZE) and Saint-Petersburg (SPB) atmospheric aerosol samples. R_I^2 , R_{II}^2 , and R_{III}^2 are the coefficients of determination of the non-linear least squares fits of the respective model Eqs. (32), (33), (34) to the experimental data.

Sample ID	k_1	R_I^2	k_2	k_3	k_4	$k_5(\text{II})$	R_{II}^2	$k_5(\text{III})$	k_6	R_{III}^2	RH_e (%)
AMAZE	0.56 ± 0.03	0.91	0.10 ± 0.01	0.003 ± 0.002	-0.011 ± 0.001	$4.9 \cdot 10^{-4} \pm 9.1 \cdot 10^{-5}$	0.98	0.186 ± 0.021	0.078 ± 0.002	0.92	64
SPB	0.51 ± 0.06	0.71	0.07 ± 0.010	-0.03 ± 0.02	-0.003 ± 0.001	$1.8 \cdot 10^{-5} \pm 4.8 \cdot 10^{-5}$	0.95	$2.6 \cdot 10^{-4} \pm 4.9 \cdot 10^{-5}$	0.047 ± 0.001	0.87	66

- [Title Page](#)
- [Abstract](#) [Introduction](#)
- [Conclusions](#) [References](#)
- [Tables](#) [Figures](#)
- [◀](#) [▶](#)
- [◀](#) [▶](#)
- [Back](#) [Close](#)
- [Full Screen / Esc](#)
- [Printer-friendly Version](#)
- [Interactive Discussion](#)

Mass-based hygroscopicity parameter interaction model

E. Mikhailov et al.

Table 4. The CCN parameters of the reference NaCl particles, and AMAZE and SPB aerosol samples. $\kappa_{m,\infty}$ is the mass hygroscopicity of the diluted droplet solution (Eq.34), ρ_d is the particle density, β is the scaling parameter and $D_{s,c}$ is the critical dry diameter estimated from Eq. (15). The critical dry diameter corresponds to the supersaturation S_w of 0.2 % and of 0.8 %.

Sample ID	$\kappa_{m,\infty}$	ρ_d (g cm^{-3})	β (nm^{-1})	$D_{s,c}$ (nm) ($S_w = 0.2\%$)	$D_{s,c}$ (nm) ($S_w = 0.8\%$)
NaCl	0.592	2.165	22.04	65.1	25.6
AMAZE	0.078	1.7	47.03	137.5	54.6
SPB	0.047	1.7	55.68	162.8	64.6

[Title Page](#)
 [Abstract](#)
 [Introduction](#)
 [Conclusions](#)
 [References](#)
 [Tables](#)
 [Figures](#)
 [◀](#)
 [▶](#)
 [◀](#)
 [▶](#)
 [Back](#)
 [Close](#)
 [Full Screen / Esc](#)
 [Printer-friendly Version](#)
 [Interactive Discussion](#)



Mass-based hygroscopicity parameter interaction model

E. Mikhailov et al.

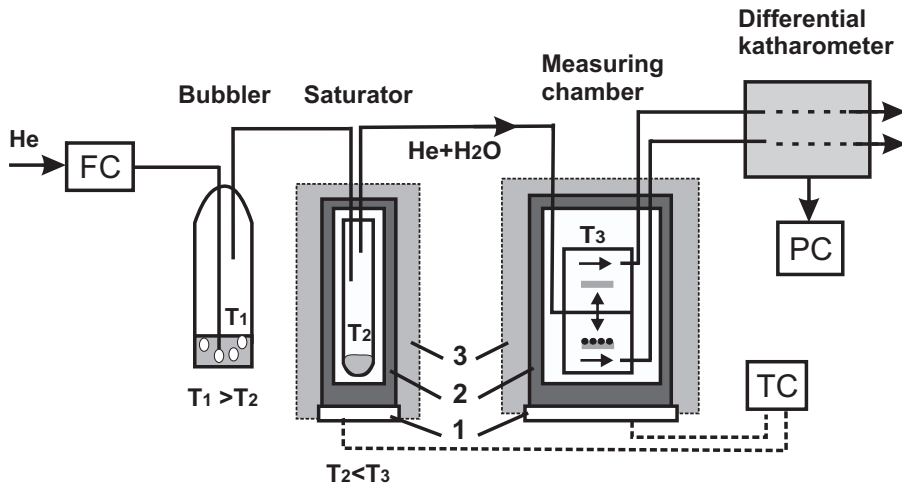


Fig. 1. Schematic set-up of the filter-based differential hygroscopicity analyzer (FDHA): FC – flow controller, TC – temperature controller, PC – computer. T_1 , T_2 , and T_3 – temperature sensors. 1-Peltier elements, 2-copper housing double wall cylinder, 3-insulation.

Title Page	Abstract	Introduction
Conclusions	References	
Tables	Figures	
◀	▶	
◀	▶	
Back	Close	
Full Screen / Esc		
Printer-friendly Version		
Interactive Discussion		

Mass-based hygroscopicity parameter interaction model

E. Mikhailov et al.

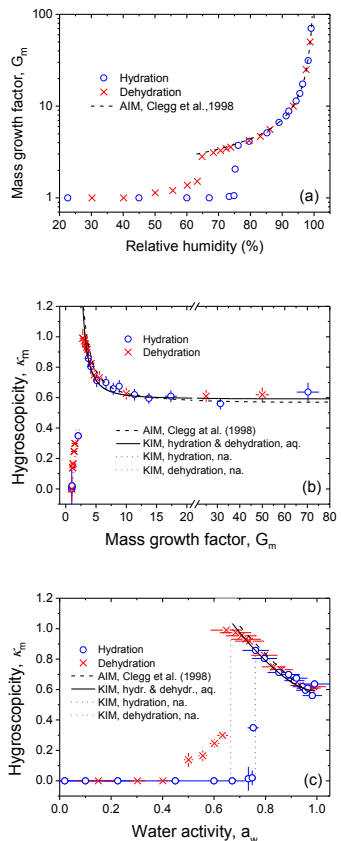


Fig. 2. Hygroscopic properties of sodium chloride (NaCl): **(a)** mass growth factors (G_m) observed as a function of relative humidity; **(b)** mass-based hygroscopicity parameters (κ_m) calculated as a function of mass growth factor (Eq. 10); and **(c)** mass-based hygroscopicity parameters (κ_m) plotted as a function of water activity. The data points and error bars are based on FDHA measurements (mean value \pm standard deviation) obtained upon hydration (blue circles) and dehydration (red crosses). The lines represent different models: AIM reference model – black dashed; KIM aqueous phase (aq) – black solid; KIM non-aqueous phase (na) equation (Eq. 27) – blue dotted for hydration and red dotted for dehydration.

Mass-based hygroscopicity parameter interaction model

E. Mikhailov et al.

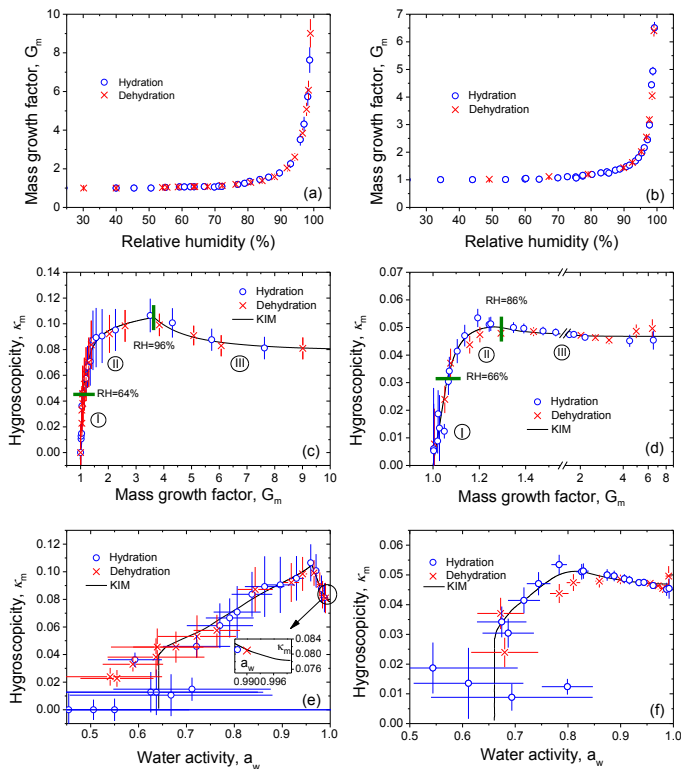


Fig. 3. Hygroscopic properties of atmospheric aerosol samples: **(a, b)** mass growth factors (G_m) observed as a function of relative humidity; **(c, d)** mass-based hygroscopicity parameters (κ_m) calculated as a function of mass growth factor (Eq. 10); and **(e, f)** mass based hygroscopicity parameters (κ_m) plotted as a function of water activity. The data points and error bars are based on FDHA measurements (mean value \pm standard deviation) obtained upon hydration (blue circles) and dehydration (red crosses). The black lines are fits of KIM Eqs. (32)–(34); the labels I, II, III indicate different regimes of hygroscopicity; and borders of the corresponding fit intervals are indicated by green lines (**(c)** and **(d)**). The left row **(a, c, e)** refers to the tropical rainforest air sample from Manaus, Brazil (AMAZE), the right row **(b, d, f)** refers to the boreal rural air sample from St. Petersburg, Russia (SPB).

Mass-based hygroscopicity parameter interaction model

E. Mikhailov et al.

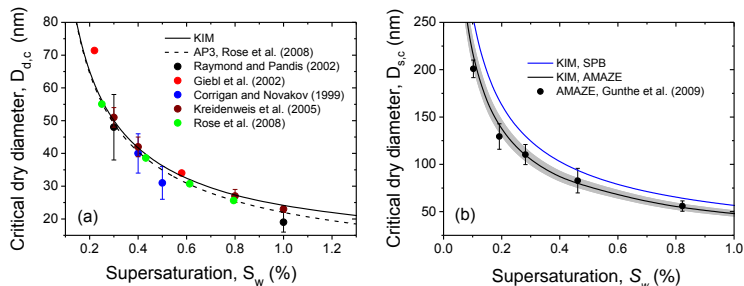


Fig. 4. Predicted critical dry diameters of CCN activation based on FDHA measurements and KIM model (Eq. 15) as compared with literature experimental data and Köhler theory with AIM water activity model (AP3, Rose et al., 2008). **(a)** NaCl particles: KIM model (black line), experimental data (colored points), Kreidenweis et al. (2005) – predicted data based on HTDMA measurements, other literature data are direct CCN measurements; **(b)** Atmospheric aerosol: KIM predicted activation dry diameters for SPB sample (blue line), and for AMAZE sample (black line); average critical dry diameters obtained from CCN measurements for AMAZE (black points with error bars; arithmetic mean \pm standard deviation). Gray shaded area denotes the estimated uncertainty in the predicted critical dry diameters for the AMAZE sample based on excursions in the particle density, where the top bound belongs to $\rho_d = 1.4 \text{ g cm}^{-3}$ and the low bound stands for $\rho_d = 2.0 \text{ g cm}^{-3}$.